Journal of
Water & Climate Change



IWA PUBLISHING



Journal of Water and Climate Change Vol 14 No 5, 1433 doi: 10.2166/wcc.2023.362

# Future water security under climate change: a perspective of the Grand River Watershed

Baljeet Kaur[a], Narayan Kumar Shrestha[a], Uttam Ghimire[a,b], Pranesh Kumar Paul[a], Ramesh Rudra[a], Pradeep Goel[a] and Prasad Daggupati [a,*]

[a] School of Engineering, University of Guelph, Guelph, ON N1G 2W1, Canada
[b] Stockholm Environment Institute Asia Center, Bangkok 10330, Thailand
*Corresponding author. E-mail: pdaggupa@uoguelph.ca

PD, 0000-0002-7044-3435

## ABSTRACT

Climate change poses a threat to the water security of the Grand River Watershed (GRW) by altering the precipitation patterns and other weather variables, which affect streamflow and freshwater availability. Therefore, in this study, a Soil and Water Assessment Tool (SWAT) model for the GRW, Ontario, Canada, was used to assess the blue and green water scarcity for future periods for future sustainable management of freshwater resources in the region. The ensemble results predicted a warmer and wetter future for the GRW. The ensemble model result, when considering both emission scenarios and future periods, showed that blue water (BW) is projected to increase by 23–40% while green water storage (GWS) is projected to experience an overall decrease (2–8%). The results suggested that BW may become more scarce compared to green water in the future. The scarcity of BW is primarily due to the projected increase in population growth and water demand in the watershed. Green water scarcity in some regions indicated that changes in irrigation might be needed in the future in some parts of the watershed. The results indicate that the careful planning is essential for future water management in GRW.

**Key words:** blue water, climate change, green water, Grand River Watershed, SWAT

## HIGHLIGHTS

- Water demand and environmental flow requirements were used to determine water scarcity.
- Green water scarcity in some regions indicated that changes in irrigation might be needed in the future in some parts of the Grand River Watershed (GRW).
- The results indicate that the careful planning is essential for future water management in GRW.

## 1. INTRODUCTION

Freshwater availability is an important requirement for the growth and development of a nation. It is not only a basic human amenity but also a primary requirement for agricultural and industrial development. The number of water resources that humans require to fulfil their daily needs is considerably less than the number of resources available in the world (Schewe *et al.* 2014), but still, in many parts of the world, the basic water needs of humans are not met (Ohlsson & Turton 1999). Various water-intensive activities, such as irrigation, sanitation, drinking, livestock farming, manufacturing goods and hydropower generation, are critical to the availability of freshwater resources (Wallace 2000). If freshwater is scarce, then the development of these activities is also threatened and hence, the socioeconomic prosperity of the region is affected as a whole (Kummu *et al.* 2010).

The freshwater scarcity problem is further aggravated by increased water demand due to population growth and dwindling water resources due to a changing climate (Parry *et al.* 2007; Faramarzi *et al.* 2013). In recent years, the impact of climate change on freshwater resources has become a major concern all around the world. It poses a threat to the water security of a region by altering the precipitation patterns and other weather variables that affect streamflow and freshwater availability (Vörösmarty *et al.* 2000; Schewe *et al.* 2014). In recent years, similar patterns have been seen in a few regions within Grand River Watershed (GRW) (Deen *et al.* 2021). As a result, in 2022, the Grand River Conservation Authority (GRCA), which manages GRW, requested the residents to reduce water consumption (Nielsen 2022). While it affects water security (the

United Nations defines Water Security as 'the capacity of a population to safeguard sustainable access to adequate quantities of acceptable quality water for sustaining livelihoods, human well-being and socioeconomic development for ensuring protection against water-borne pollution and water-related disasters, and for preserving ecosystems in a climate of peace and political stability'), it also influences the ability of a region to harness water for enhancing food security (Vörösmarty *et al.* 2000). Therefore, it is necessary to seek some innovative options to meet the challenges posed by climate change. One method could be to study the spatial and temporal distribution and variation of available freshwater resources and water scarcity in future periods (Veettil & Mishra 2016). This analysis, if performed at finer spatial resolutions, can guide various climate change adaptations and alleviation operations (Faramarzi *et al.* 2013).

There are numerous studies that have focused only on quantifying the freshwater resource components (blue and green water) [blue water (BW) is the water in our surface and groundwater reservoirs. On the other hand, green water is the water transpired by the plant that comes from rainwater stored in soil] (Gosling *et al.* 2011; Abbas *et al.* 2016a, 2016b). Only a few of the studies projected the water scarcity situation (Schewe *et al.* 2014; Veettil & Mishra 2018). Moreover, many scientists did not focus on using simplistic indicators to estimate water scarcity (Schewe *et al.* 2014). The studies, which have used more refined indicators, such as blue and green water scarcity (Veettil & Mishra 2018), did not project future climate change impacts on freshwater resources. Few studies, which did project future climate change impacts (Schewe *et al.* 2014) did not use a complete and refined indicator that incorporated green water resources and environmental flow requirements (EFRs).

In these circumstances, the main aim of the study was to project the impact of future climate on freshwater resources and water scarcity in the GRW in southwestern Ontario, Canada, using a simple water scarcity indicator. For this study, the water footprint-based scarcity indicator was chosen. But it should be noted that the estimates of future climate impact not only depend on the assumed scenario but also on the projected population for that future scenario. For this purpose, population projections were obtained from shared socioeconomic pathways (SSPs) (Riahi *et al.* 2017) and incorporated into the analysis. Meanwhile, the study is the first at GRW, if not at other parts of the world, to the best of the authors' knowledge. Thus, the results can form a basis for various climate change adaptation and mitigation strategies, which could guide various water management and policy decisions in GRW.

## 2. MATERIALS AND METHODS

### 2.1. Study area and data

The GRW lies in southwestern Ontario, Canada (Figure 1) and flows into Lake Erie, draining a total of over 6,500 km$^2$ area. In its 310 km long route, it is drained by four major tributaries: the Conestoga, the Nith, the Eramosa and the Speed Rivers (Zhang *et al.* 2018). The GRW comprises agricultural lands (43%), pasture and range grasses (27%), forests (12%) and small fragments of urban areas (9%) and wetlands (2%). The GRW has a moderate to cool temperate climate with annual average precipitation ranging between 800 and 900 mm and temperatures between 8 and 10 °C (Kaur *et al.* 2019).

For analysis, the GRW was discretized into eight spatial zones based on the rivers draining to the Grand River (Kaur *et al.* 2019). Zone A (the Grand River Headwaters sub-watershed) lies in the headwater region and has mostly agricultural (37%) and pasture lands (32%). This zone has the only wetland located in the GRW. Zone B is also a headwater region and is mostly forested. Zone C receives inflow from Zone A and has mostly agricultural lands (52%). Zones D and G are highly urbanized and lie in the central part of the GRW. Some high population-centric cities like Guelph, Kitchener, Cambridge and Waterloo are located in these zones. Zones E, F and H are in the lowermost part of the GRW and are mostly cultivated (53, 35 and 44%) and have few patches of pastures (25, 31 and 23%) and population centres (5, 8 and 8%). The details of the data have been described in Supplementary material, Table S1.

### 2.2. The Soil and Water Assessment Tool

The Soil and Water Assessment Tool (SWAT) is an integrated, process-based and semi-distributed hydrological model that comprises a plant-growth simulation module and works on a daily time-step (Arnold *et al.* 1998; Schuol *et al.* 2008). SWAT has been used by various researchers all around the world (Gassman *et al.* 2007) to study water quality (nutrients and sediments), water quantity (water availability), crop growth, climate change impact assessment (Faramarzi *et al.* 2013; Veettil & Mishra 2016), water scarcity studies (Abbaspour *et al.* 2015; Veettil & Mishra 2016) in large watersheds having varying soils, land-covers and management practices. The details on model setup, calibration and validation are provided in Supplementary material, Section 1.

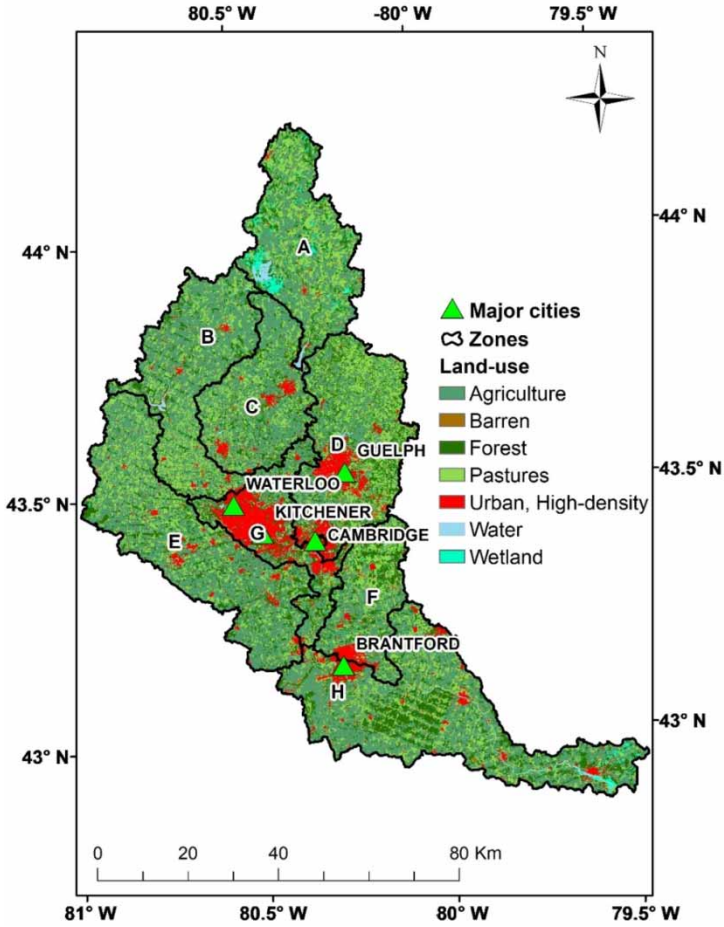


**Figure 1** | The GRW with major cities and eight different zones. (GRW with the Digital Elevation Model (DEM), the six gauging stations and the river network derived from the DEM are shown in Supplementary material, Figure S1.)

### 2.3. Global climate models

The selection of a Global Climate Model (GCM) capable of simulating historical rainfall and its seasonality over a region of interest is crucial in climate change impact assessments (Ghimire *et al.* 2019). For the Eastern North America (ENA) region, Murdock *et al.* (2013) have shortlisted the top 12 GCMs from Coupled Model Intercomparison Project Phase 5 depending on prediction accuracy (Taylor *et al.* 2012). Of these 12 GCMs, the top three GCMs are MPI-ESM-LR (Giorgetta *et al.* 2013), INMCM4 (Volodin *et al.* 2010) and CNRM-CM (Voldoire *et al.* 2013). Thus, this study uses the projected data of these three models, downloaded from the Pacific Climate Impact Consortium (PCIC) 2014, at a gridded resolution of 300 arcseconds (approximately 10 km). The projected data included bias-corrected and spatially (statistically) downscaled daily precipitation and minimum and maximum temperatures for the 2035–2100 period for two emission scenarios of representative concentration pathways, RCP4.5 and RCP8.5.

In this study, the coarse-resolution input data were downscaled by PCIC( 2014) using two statistical techniques: Bias-Correction Spatial Disaggregation (BCSD) and Bias-Correction Analogues with Quantile mapping reordering (BCCAQ). The BCSD produces downscaled grids of finer resolution by using quantile mapping for bias-correction and relating the GCM prediction quantiles to historical patterns and then disaggregating to daily time-step (Maurer & Hidalgo 2007). The BCCAQ, on the other hand, is a hybrid tool that aggregates the results obtained from Bias-Corrected Constructed Analogues (BCCA) (Maurer *et al.* 2010) and quantile mapping (Gudmundsson *et al.* 2012). The BCCA uses a similar methodology as is used in the BCSD, but it obtains the spatial information for each grid by combining the historical analogues linearly. The downscaled GCM projections were calibrated using historical data from 1950 to 2005 (PCIC 2014).

The gridded climate data obtained from these GCMs was then fed to the calibrated and validated SWAT model (Kaur *et al.* 2019) for the GRW. The outputs obtained from the hydrological model were then used to estimate the spatial and temporal

trend of blue and green water resources and water scarcity. We have presented the comparison of the bias-corrected GCM simulations with the observed data in Section 2.1 (Supplementary material). Then, we analysed different combinations of GCMs, bias-correction techniques and RCP scenarios with the observed data (Supplementary material, Section S2.1). We found the results are almost similar and it was hard to differentiate the best combination. Hence, we have decided to consider all the combinations and infer the results mainly with the ensemble. We again advocate the use of 'ensemble' to deal with different sources of uncertainty. As the study included two RCP scenarios for three GCMs, downscaled using two different techniques and for two time periods by PCIC (2014), the hydrological model was run, in total, 24 times to estimate the freshwater resources and water scarcity for the ensemble.

### 2.4. Quantification of BW and green water resources and scarcity

BW was estimated as the sum of water yield and deep-aquifer recharge from a particular sub-basin (Rodrigues *et al.* 2014). The water yield is defined as the total amount of water leaving a sub-basin and flowing into the main channel and the deep-aquifer recharge is the amount of water that moves from the land surface or vadose zone to recharge the saturated zone of the soil (deep-aquifer) (Nimmo 2009). Water yield was obtained from SWAT sub-basin output files and deep-aquifer recharge was extracted from the hydrologic response units (HRUs) output files.

Green water resources are a combination of green water flow (GWF) (evapotranspiration) and green water storage (GWS) (soil moisture) (Schuol *et al.* 2008). Both evapotranspiration and soil moisture content were obtained from the SWAT output table at the sub-basin scale.

BW scarcity was estimated as the ratio of the consumptive use of BW and the available blue water ($BW_{available}$). The BW used for the baseline analysis was obtained from the Water Use Inventory Report for the GRW (Wong 2011). The water use was divided into agricultural, municipal, recreational, dewatering, industrial and remediation purposes. The major water use sector was municipal (60.83%), followed by water removed for dewatering (6.07%), agricultural (4.47%) and agricultural livestock (4.41%) (Wong 2011). For estimating the consumptive use of BW under climate change scenarios, future water use data were required. Since this data were not readily available and needed a lot of complex statistical analysis, it was roughly estimated from future population growth data obtained from SSP (Riahi *et al.* 2017). SSPs are developed by the climate change research community to support the integrated analysis of climate change impacts, adaption and alleviation. There are five SSP storylines or scenarios that describe various alternative socioeconomic development pathways. For this study, SSP2 or the intermediate scenario was chosen, which assumed a middle-of-the-road scenario consistent with past development patterns (Supplementary material, Figure S8).

Various studies in the literature supported the notion that domestic or municipal water use rises proportionally with the population if the per capita use remains the same (Hoffman 2007; Miro *et al.* 2018) while, the commercial, industrial and residential water use may increase at a higher rate than the population (Hoffman 2007). In GRW, the major water use sector was municipal, which accounted for around 61% of the total water used, so it was assumed that water demand also increased approximately at the same rate as the population. The population growth-rate data were obtained from the SSP2 database (Samir & Lutz 2017) for Canada at every 5-year interval from 2035 to 2099 and the same percent rise was assumed for water use. To be specific, the base for predicting future water use information was the data available for the year 2008 from the Wong (2011) report (https://www.grandriver.ca/en/our-watershed/resources/Documents/Water_Supplies_WaterUse_2011.pdf).

$BW_{available}$ is the limited amount of water that can be extracted from a surface or groundwater resources without affecting their ecological balance. To maintain ecological balance, a certain share of water in the water bodies must be saved for EFRs. Various approaches are available to estimate the share of the environment in the water body. However, in this study, the variable monthly flow method was used to estimate the EFR. It is a parametric method of EFR estimation and was proposed by Pastor *et al.* (2014). This method considers the natural variability of the flow by considering EFR at a seasonal scale. It classifies the flow into three classes: low flow (mean monthly flow (MMF) $\leq$ 40% of the mean annual flow (MAF)) for which the EFR = 0.6 MMF, intermediate flow (40% of MAF < MMF < 80% of MAF) for which the EFR = 0.45 MMF and high flow (MMF > 80% of MAF) for which the EFR = 0.3 MMF. The $BW_{available}$ is then calculated as in the following Equation (1):

$$BW_{(available)(x,t)} = Q_{(x,t)} - EFR_{(x,t)} \quad (1)$$

where, $EFR_{(x,t)}$ is the environmental flow requirement for drainage area '$x$' at time '$t$' and $Q_{(x,t)}$ is the corresponding streamflow in $m^3/s$. The percentage change of annual environmental flow requirements (EFRs) in two future periods under two emission scenarios, relative to the base-period (1950–2015), has been shown in Supplementary material, Table S6.

Green water scarcity is the ratio of the green water footprint (evapotranspiration) to available green water (soil moisture) (Hoekstra *et al.* 2012). Both the green water footprint and available green water were obtained from SWAT output files for various scenarios. Green water footprint or evapotranspiration was simulated using the Hargreaves method (Hargreaves *et al.* 1985). It is calculated as in the following Equation (2):

$$GW_{\text{scarcity}} = \frac{GW_{\text{footprint }(x,t)}}{GW_{\text{available }(x,t)}} \tag{2}$$

where $GW_{\text{footprint }(x,t)}$ is the amount of green water consumed or evapotranspiration in zone '$x$' during the time '$t$' and $GW_{\text{available }(x,t)}$ is the initial soil water content present in zone '$x$' for time '$t$'.

The summary of the methodology workflow has been shown in Figure 2.

## 3. RESULTS AND DISCUSSION

The calibrated and validated SWAT model has been ready for further analysis (Kaur *et al.* 2019). Therefore, we have used the model for further analysis in this study, following the methodology in Sections 2.3 and 2.4 as well as Figure 2. The results are presented below. However, we have skipped the results of SWAT model calibration and validation, as they have already been represented in Kaur *et al.* (2019).

### 3.1. Climate change projections

The weather in the GRW, in the future period, is expected to be wetter and warmer. Mainly, the high-emission scenario (RCP 8.5) in the late century was found to be the wettest and warmest, using both downscaling methods (Figure 3). However, significant spatial (Supplementary material, Figures S9 and S10) and temporal (Supplementary material, Table S4 and Figure S11) variability was observed in the projections across the GRW and noticeable differences in the projections of different climatic models were observed. It was found that the climate change impacts were climate model, emission scenario and chosen-downscaling-method-specific.

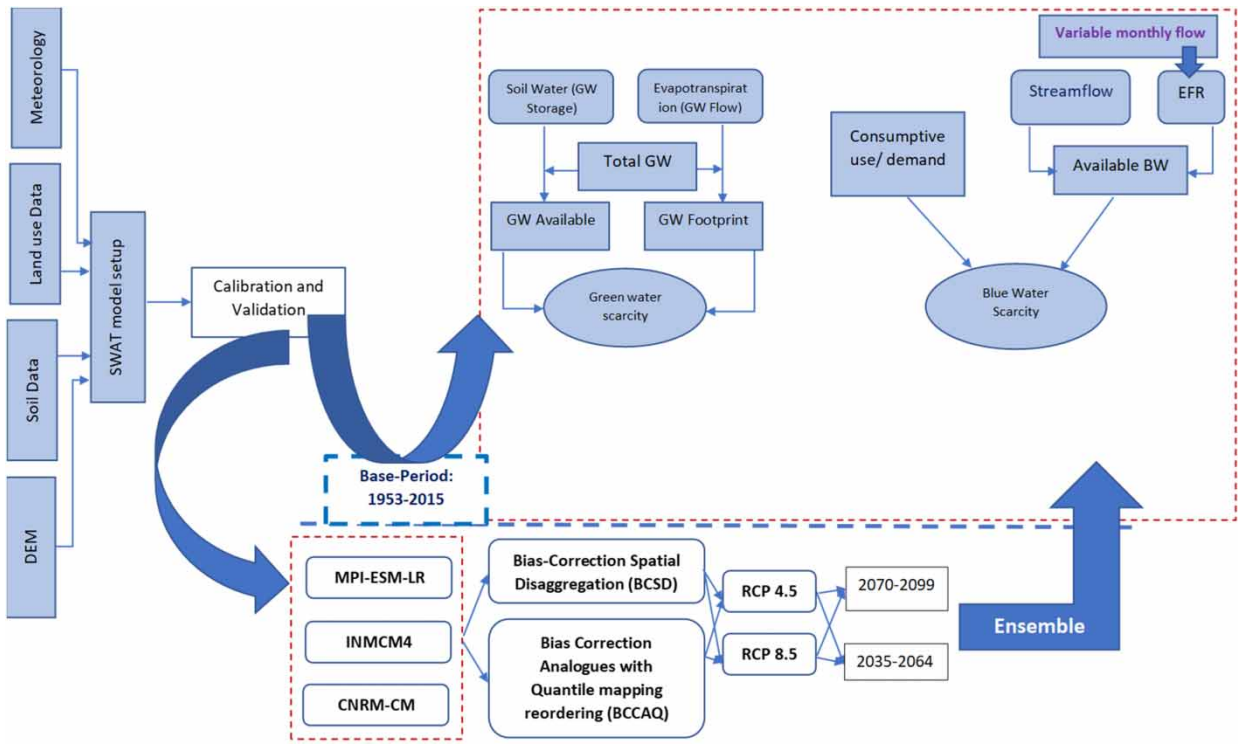


**Figure 2** | Flowchart of the methodology of the study.

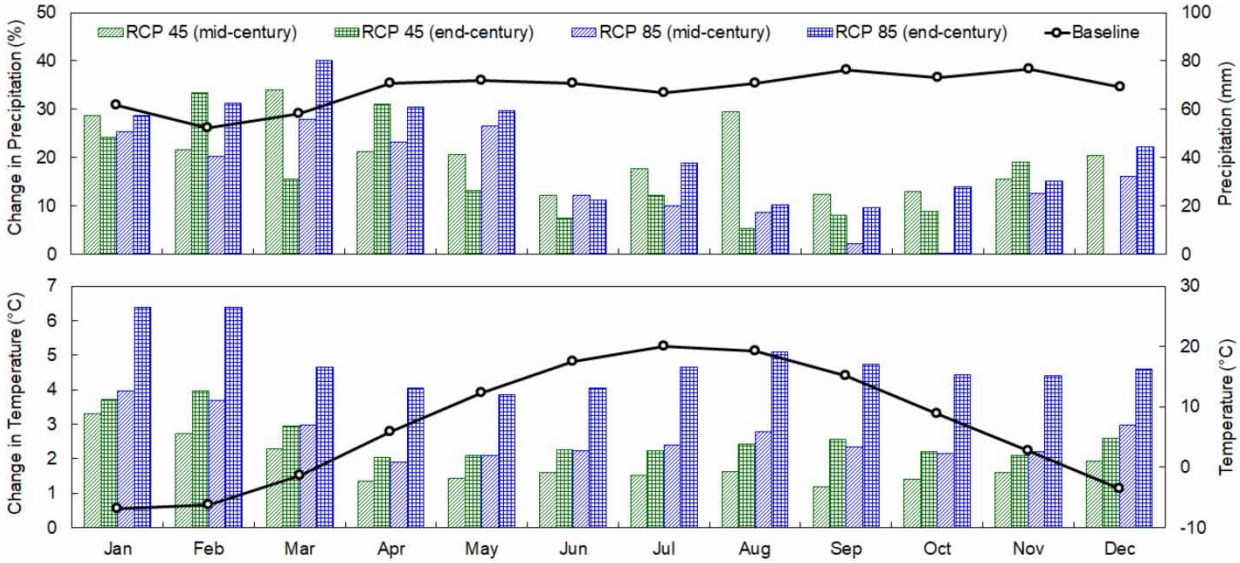


**Figure 3** | Percentage change in monthly precipitation and absolute change in monthly temperature of the GRW between the base-period (1950–2015) and two future periods (2035–2064 and 2070–2099) under two emission scenarios.

It was observed that significant intra-annual variability existed in the climate change projections. The ensemble results projected a higher precipitation increment in the winter months (January–April) and a lower increment in the summer and early fall months (June–September), under emission scenarios. Similarly, for temperature, the increments were higher in the winter months (January–March) and relatively lower in the summer and fall (May–October). Consequently, GRW can expect early snowmelt caused by warmer winters because of global warming. No other similar studies have been performed in GRW. However, a similar trend was observed by Shrestha & Wang (2018b) in the Athabasca River Basin in Alberta, Canada.

The ensemble results also exhibited a wetter future, with a significantly increasing trend in both mid- and end-century periods. MPI-ESM-LR and CNRM-CM-based predictions were observed to be wetter and warmer as compared to INMCM-based projections (Supplementary material, Table S4). The precipitation is projected to increase by 6–27% and 9–28% in the mid- and end-century periods, respectively, based on the emission scenarios and climate models (Supplementary material, Table S4). The highest precipitation increase was projected by MPI-ESM-LR in the end-century period under the RCP 8.5 scenario and the lowest by INMCM4 in the mid-century period under the RCP 8.5 scenario. The projected percentage changes were consistent with other climate change studies done in other cold-climate Canadian watersheds (Sanderson 1993; Li *et al.* 2016; Shrestha *et al.* 2017; Shrestha & Wang 2018a; Zhang *et al.* 2018). Similarly, the temperature increments projected by the three models also showed marked variability following the same trend (Supplementary material, Table S4). The GRW was projected to be the warmest in the end-century period under the RCP 8.5 emission scenario. Relative to the base-period (1950–2015), the annual average temperature was projected to increase from 1.13 to 2.42 °C under the RCP 4.5 emission scenario and from 1.61 to 3.42 °C under the RCP 8.5 emission scenario in the mid-century period (Supplementary material, Table S4). Further, temperature values were projected to increase from 1.72 to 3.30 °C and from 3.31 to 6.02 °C in the end-century period in the two emission scenarios (Supplementary material, Table S4). Similar warming trends in the GRW were also reported by (a) Shifflett (2014), who reported mean monthly temperature increases up to 2.8 °C; (b) Sanderson (1993), who reported changes in mean temperature in the range between 4.7 and 5.7 °C; and (c) Li *et al.* (2016) who reported increases between 6.1 and 8.3 °C.

Regarding the spatial representation of climate change impact projections, for all 24 scenarios for the GRW, it was observed that for a given GCM and emission scenario, the percentage increment in precipitation was approximately the same across the GRW, with very little inter-zonal variation (4–5% across the whole GRW; Supplementary material, Figure S9). The precipitation increment decreased while moving from the upstream zones (Zones A and B) to the downstream areas (Zones F and H). Similarly, the variation in the temperature increment across the GRW was also very less (from <0.5 to 1 °C, Supplementary material, Figure S10) for a given GCM and emission scenario. Higher temperature

increments were observed in the Nith River sub-watershed (Zone E). A similar spatial pattern was also reported by Li *et al.* (2016) over the GRW.

### 3.2. Climate change impact on freshwater resources

The climate models predicted an overall increase in BW resources, which was mainly driven by an overall increase in precipitation. At a finer spatio-temporal scale, the BW availability was found to be predominantly higher in the winter months (January–April) due to the shifting of peak flow from April to March. As discussed in the previous section, this shift in peak flow was caused by an overall increase in winter temperatures due to increased air temperatures in the winter months. During June–September, the increase in precipitation was offset by an increase in temperature, which resulted in the relatively same amount of BW as obtained in the base-period.

While there existed marked variability in the projected BW resources as per climate models, downscaling techniques and emission scenarios, the ensemble result indicated significant increasing trends in both the mid-century (Sen's slope = 4.7 mm/decade, $p < 0.05$) and end-century (Sen's slope = 4.1 mm/decade, $p < 0.05$) periods. MPI-ESM-LR and CNRM-CM5 projected similar results and predicted an increase from 41 to 68% and from 43 to 65% (Supplementary material, Table S5), respectively, for the mid-century period and low-emission scenario (RCP 4.5) and from 20 to 46% and from 21 to 43% in the end-century period. A similar pattern of increased BW was observed in the high-emission scenario as well. The INMCM4 followed the same pattern, but with smaller changes projected for future scenarios (2035–64 and 2070–99). In some zones (Zones E and H), even a decrement was projected by INMCM4.

The spatial changes in annual BW resources for the two emission scenarios and two future periods for eight zones of GRW are presented in Supplementary material, Table S5, Figure 4(a) and Supplementary material, Figure S12. It was observed that the variation in BW resources was dependent on climate model projections of precipitation and temperature and that the effects of precipitation and temperature were either synergetic or offsetting (Shrestha *et al.* 2017). For instance, in the headwater sub-watersheds (Zones A, B) and the Speed and Eramosa River sub-watersheds (Zone D), temperature increment was lower and precipitation increment was higher, thus resulting in an overall increase in BW in the three zones. Similarly, the

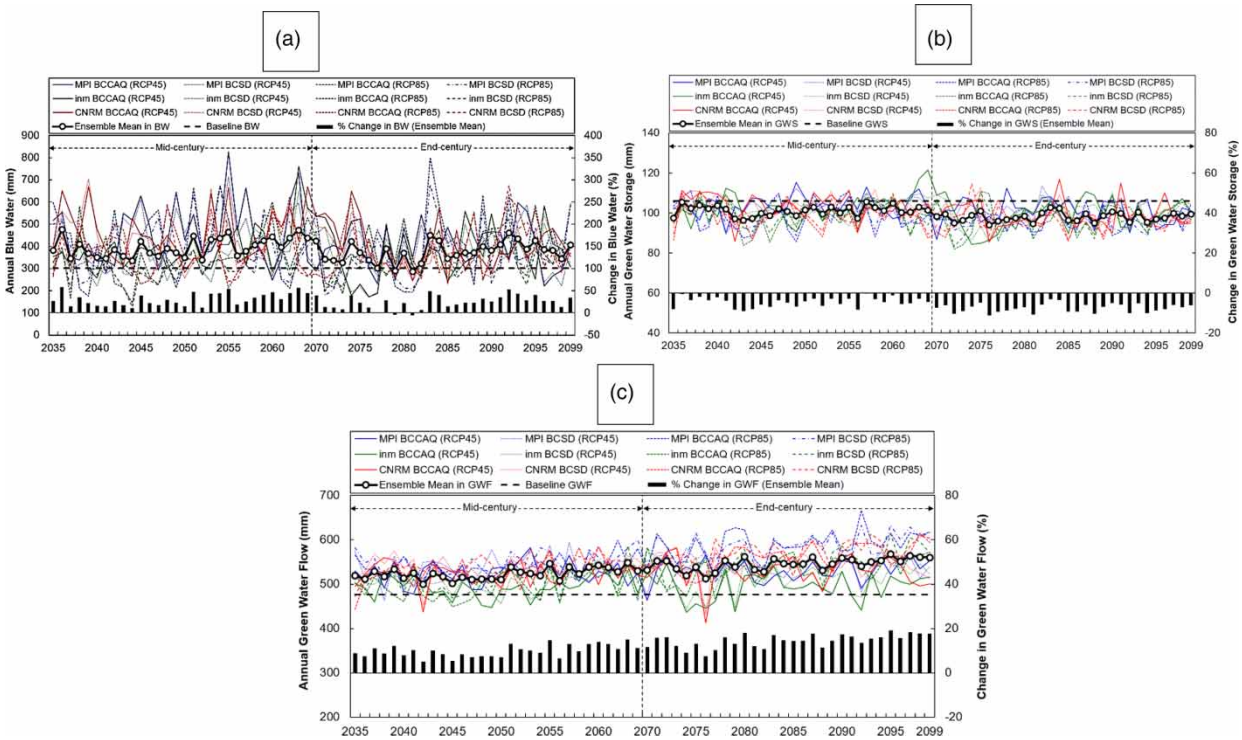


**Figure 4** | (a) Annual BW of the GRW; (b) annual GWS of the GRW; and (c) annual GWF of the GRW, in the base-period (as dotted horizontal line) and two future periods (as thin lines for individual climate models and thick line with markers for the model ensemble). Also shown is the percentage change (as vertical bars) in the annual BW between the base-period (1950–2015) and two future periods.

west-southern part of the GRW (Zones E, H) is projected to experience a decrease in BW due to a lower increment in precipitation and a higher increment in temperature, more prominently for the high-emission scenario.

Similarly, the ensemble results predicted a non-significant decrease in GWS and a significant increase in GWF. It was observed that in the summer months (June–August), GWS was the lowest on account of higher crop-water demand and GWF was the highest due to high temperatures. Also, in May, the seeds sown would have barely grown in the agricultural lands (as most of the crops are sown at April-end or at the beginning of May), thus exposing the bare surface of the soil and enhancing the rate of soil evaporation as well. In the fall and winter months (October–April), the GWF was projected to reach its minimum and the GWS was expected to reach its maximum due to precipitation increment.

The spatial representations of GWS and GWF for each zone and under different future periods of both the emission scenarios and downscaling techniques are presented in Figure 4(b) and 4(c). Most of the GCMs were consistent in simulating the decrease in GWS for both the mid-century (from 0.5 to 8%) and end-century (from 0.9 to 13%) periods under the low-emission scenario (Supplementary material, Table S5). Few spatial zones even showed percentage increments in the GWS ranging from 0.5 to 3%. Under the high-emission scenario, GCMs were consistent in simulating the decrease in GWS (up to 16%). For GWF, all GCMs were unidirectional in projecting the increase for both the mid-century (from 2 to 16%) and end-century (from 2.5 to 18%) periods under the low-emission scenario. Under the high-emission scenario, the increments in GWF reach up to 29%. The increases in GWF for the mid-century (Sen's slope = 1.4 mm/decade, $p < 0.05$) and end-century (Sen's slope = 1.7 mm/decade, $p < 0.05$) periods explain the corresponding lower percentage increase in BW availability in the end-century period.

Spatial changes in GWS and GWF are shown in Supplementary material, Figures S13 and S14. Zone E showed the maximum percentage increase in GWF and the maximum percentage decrease in GWS. Minimal increases in GWS were observed in Zones B, C and some parts of Zone D due to the minimal reduction in corresponding GWF, especially for low-emission

**Table 1** | Percentage change of available blue water scarcity in two future periods under two emission scenarios, relative to the base-period (1950–2015)

| Zones | Models | Baseline | RCP 4.5 (Mid) (%) | RCP 4.5 | RCP 8.5 (Mid) (%) | RCP 8.5 |
|---|---|---|---|---|---|---|
| A | MPI-ESM-LR | 0.09 | 272 | 433 | 269 | 430 |
| | inmcm4 | | 422 | 536 | 330 | 192 |
| | CNRM-CM5 | | 292 | 519 | 532 | 694 |
| B | MPI-ESM-LR | 0.09 | 271 | 366 | 265 | 418 |
| | inmcm4 | | 304 | 590 | 297 | 119 |
| | CNRM-CM5 | | 250 | 456 | 532 | 710 |
| C | MPI-ESM-LR | 0.11 | 317 | 393 | 223 | 459 |
| | inmcm4 | | 348 | 587 | 322 | 154 |
| | CNRM-CM5 | | 272 | 515 | 513 | 714 |
| D | MPI-ESM-LR | 0.65 | 250 | 420 | 247 | 498 |
| | inmcm4 | | 359 | 530 | 301 | 172 |
| | CNRM-CM5 | | 270 | 569 | 588 | 701 |
| E | MPI-ESM-LR | 0.40 | 187 | 331 | 177 | 246 |
| | inmcm4 | | 280 | 394 | 208 | 90 |
| | CNRM-CM5 | | 207 | 293 | 363 | 502 |
| F | MPI-ESM-LR | 0.07 | 178 | 301 | 148 | 219 |
| | inmcm4 | | 278 | 277 | 189 | 123 |
| | CNRM-CM5 | | 181 | 293 | 286 | 448 |
| G | MPI-ESM-LR | 0.18 | 222 | 294 | 181 | 327 |
| | inmcm4 | | 245 | 414 | 217 | 123 |
| | CNRM-CM5 | | 205 | 373 | 403 | 543 |
| H | MPI-ESM-LR | 0.07 | 156 | 240 | 132 | 259 |
| | inmcm4 | | 195 | 313 | 239 | 97 |
| | CNRM-CM5 | | 157 | 280 | 313 | 412 |
| Watershed | All models | 0.21 | 255 | 405 | 303 | 360 |

scenarios. The soil depth is also quite high in these zones, which may contribute to the gradual reduction of GWF and corresponding increases in GWS. An assessment of Zone H revealed a decrease in both GWF and GWS for future scenarios. These reductions were accompanied by higher increments in BW availability, which could be due to the frequent, short-term and intense rainfall events.

A synopsis of future predictions shows that freshwater resources in GRW are likely to change, which can be crucial for various sectors. For example, hydropower projects dependent on BW may be benefitted from increasing BW, while agriculture dominant zones of GRW may need alternative sources of replenishing soil moisture. These changes are a cumulative impact of soil characteristics and changing precipitation and temperature patterns across different zones of the GRW.

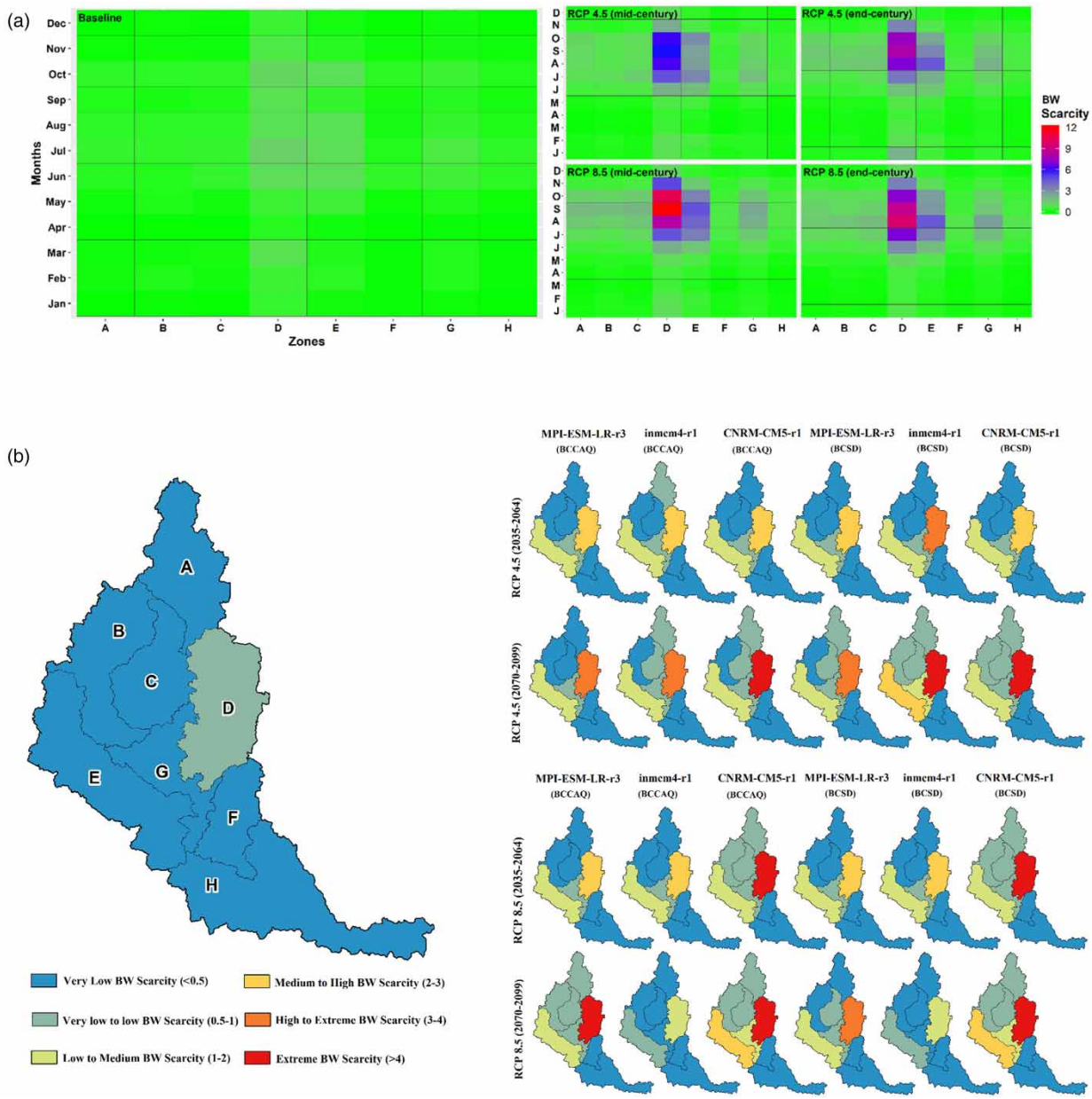


**Figure 5** | (a) Monthly BW scarcity heat maps at different zones of the GRW for two emission scenarios and during two future periods and (b) spatial variation of percentage change in available annual BW scarcity relative to the base-period (1950–2015), in two future periods (2035–2064 and 2070–2099) and under two emission scenarios.

### 3.3. Climate change impact on BW scarcity

The analysis shows an overall increasing trend of BW scarcity for both emission scenarios. Precisely, this study used the concept of water footprint to evaluate BW scarcity, which considers both supply and demand sides. The supply side is stressed due to the variations in BW availability and the demand side is stressed due to the increasing population and the related socio-economic developments (Schewe *et al.* 2014).

The ensemble of climate models suggested marked heterogeneity of BW scarcity among different zones of GRW under future scenarios. It was observed that the usual month when BW scarcity was at its maximum during baseline (July) shifts to August/ September during future periods. These changes ranged from 255 to 405% for the entire GRW (Table 1) and

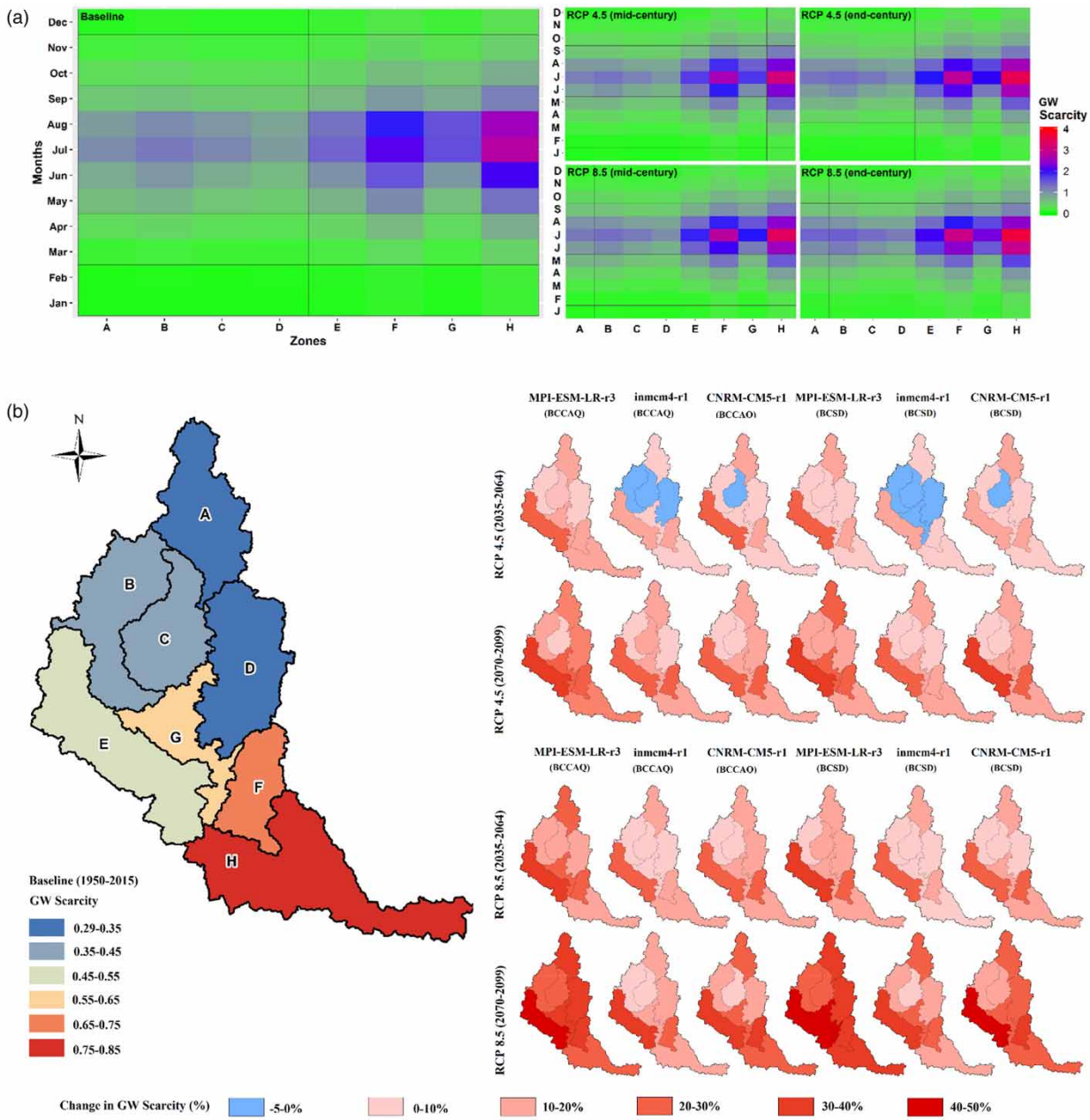


**Figure 6** | (a) Monthly GW scarcity heat maps at different zones of the GRW for two emission scenarios and during two future periods and (b) spatial variation of percentage change in available annual GW scarcity relative to the base-period (1950–2015), in two future periods (2035–2064 and 2070–2099) and under two emission scenarios.

are much more significant at the zonal level. Zone D, for example, has some urban centres and has lower BW resources given its location in the headwaters of the GRW and is thus projected to have severe BW scarcity (see Figure 5(a) and Supplementary material, Figures S15 and S18). Similarly, Zone G has significant urban centres and the corresponding highest water demand in the GRW, but the severity of BW scarcity is lower due to the contribution from the upstream sub-basins. Another sub-watershed that projected high BW scarcity was Zone E, due to lower GWS, higher GWF and ultimately lower available BW. The spatial representation of BW scarcity for each zone under different future periods of both scenarios and bias-correction techniques is presented in Figure 5(b).

Despite all climate models exhibiting an increase in BW scarcity for different zones of the GRW, significant variabilities are observed between climate models, emission scenarios and future periods (Table 1). The range of increase varied from 132 to 588% during mid-century and from 90 to 714% during end-century periods, with prominence under the high-emission scenario of all climate models. Given the lower magnitudes of baseline BW scarcity values, the percentage of projected changes was significantly overwhelming.

### 3.4. Climate change impact on green water scarcity

The increment of GW scarcity for the GRW was found to be lower than that of BW (Figures 5(a), 6(a) and Supplementary material, Figures S19). At finer spatio-temporal resolution, GW scarcity was found to be dominant during June–August under both baseline and future scenarios due to a higher GW footprint (i.e., GWF). However, the severity of GW scarcity is found to increase under both lower and higher emission scenarios for Zones F–H. Correspondingly, the lowest GW scarcities are projected for the winter months (i.e., December–February), when the GWS is maximum (Supplementary material, Figure S16) and the GWF is minimum (Supplementary material, Figure S17).

A moderate inter-model variability of GW scarcity for future scenarios is presented in Table 2. Mostly, all GCMs projected an overall increase in GW scarcity with values ranging from −4 to 32% and from 2 to 49% for low and high-emission

**Table 2** | Percentage change of available GW scarcity in two future periods under two emission scenarios, relative to base-period (1950–2015)

| Zones | Models | Baseline | RCP 4.5 (Mid) (%) | RCP 4.5 | RCP 8.5 (Mid) (%) | RCP 8.5 |
|---|---|---|---|---|---|---|
| A | MPI-ESM-LR | 0.41 | 13 | 20 | 21 | 37 |
| | inmcm4 | | 6 | 13 | 11 | 21 |
| | CNRM-CM5 | | 10 | 18 | 17 | 29 |
| B | MPI-ESM-LR | 0.48 | 4 | 10 | 10 | 24 |
| | inmcm4 | | −2 | 4 | 3 | 10 |
| | CNRM-CM5 | | 1 | 8 | 8 | 17 |
| C | MPI-ESM-LR | 0.40 | 2 | 9 | 9 | 23 |
| | inmcm4 | | −4 | 2 | 1 | 9 |
| | CNRM-CM5 | | 0 | 7 | 6 | 15 |
| D | MPI-ESM-LR | 0.36 | 7 | 15 | 14 | 32 |
| | inmcm4 | | −2 | 6 | 3 | 14 |
| | CNRM-CM5 | | 4 | 11 | 10 | 20 |
| E | MPI-ESM-LR | 0.53 | 24 | 33 | 32 | 49 |
| | inmcm4 | | 16 | 26 | 24 | 32 |
| | CNRM-CM5 | | 20 | 30 | 28 | 40 |
| F | MPI-ESM-LR | 0.83 | 17 | 25 | 24 | 38 |
| | inmcm4 | | 10 | 20 | 17 | 25 |
| | CNRM-CM5 | | 15 | 24 | 22 | 31 |
| G | MPI-ESM-LR | 0.59 | 10 | 22 | 19 | 39 |
| | inmcm4 | | 0 | 11 | 7 | 21 |
| | CNRM-CM5 | | 4 | 17 | 13 | 28 |
| H | MPI-ESM-LR | 1.07 | 10 | 19 | 16 | 29 |
| | inmcm4 | | 3 | 14 | 11 | 18 |
| | CNRM-CM5 | | 7 | 16 | 15 | 23 |
| Watershed | All models | 0.58 | 7 | 16 | 14 | 26 |

scenarios, respectively. As GW scarcity is largely dependent on GWF, it followed the projected pattern of GWF for the GRW. The decreasing values of GW scarcity were observed in the same sub-watersheds, where GWS values were projected to increase in the future. It is quite understandable, as the relationship between GW scarcity and GWS is inverse, as discussed in the methodology section.

Figure 6(b) shows the spatial variation of GW scarcity during the base-period (1950–2015) and for future periods as projected by various climate models and emission scenarios. The maximum percentage increase was projected in Zones E and F due to the corresponding increases and decreases in GWF and GWS, respectively. Also, Zones B and C experienced a decrease in GW scarcity, which can be attributed to an increase in GWS in the respective sub-watersheds. It is expected that Zones B and C will be able to self-sustain rain-fed agriculture, while Zones E and F will either require changes in irrigation or agricultural practices to adapt with changing climate.

## 4. CONCLUSIONS

In this study, a previously calibrated and validated SWAT model against observations at multiple sites of the GRW was used to analyse the impact of climate change on blue and green water resources and the water security of the watershed. Climate change projections from three climate models, two emission scenarios and two future periods were used for this purpose. Overall, the ensemble results projected a wetter and warmer future for the watershed. Some specific conclusions are as follows (Kaur *et al.* 2019):

- The ensemble results projected an overall increase in BW resources.
- The ensemble projected an overall increase in GWF and an overall decrease in GWS.
- BW scarcity exhibited a significant increase with marked variability between different zones in the watershed.
- Green water scarcity exhibited an overall increase with lesser prominence compared to BW.

The modeling results presented in this paper as based on assumptions and simplifications as discussed earlier. Readers should be careful when interpreting our modeling results and should consult with experts and stakeholders before applying our results to any specific context or problem.

## ACKNOWLEDGEMENTS

We would like to thank Natural Sciences and Engineering Research Council (NSERC) for providing the funding support for this research. We would also like to acknowledge Dr Rituraj Shukla, Jun Hou, Nabil Allataifeh, Fahimeh Jafarianlari, and Harshpinder S. Brar for their insights and comments, which helped to shape the manuscript.

## DATA AVAILABILITY STATEMENT

Data cannot be made publicly available; readers should contact the corresponding author for details.

## CONFLICT OF INTEREST

The authors declare there is no conflict.

## REFERENCES

Abbas, N., Wasimi, S. A. & Al-Ansari, N. 2016a Climate change impacts on water resources of Greater Zab River, Iraq. *Journal of Civil Engineering and Architecture* **10**, 1384–1402.

Abbas, N., Wasimi, S. A. & Al-Ansari, N. 2016b Impacts of climate change on water resources in Diyala River Basin, Iraq. *Journal of Civil Engineering and Architecture* **10**, 1059–1074.

Abbaspour, K. C., Rouholahnejad, E., Vaghefi, S., Srinivasan, R., Yang, H. & Kløve, B. 2015 A continental-scale hydrology and water quality model for Europe: calibration and uncertainty of a high-resolution large-scale SWAT model. *Journal of Hydrology* **524**, 733–752.

Arnold, J. G., Srinivasan, R., Muttiah, R. S. & Williams, J. R. 1998 Large area hydrologic modeling and assessment part I: model development. *Journal of the American Water Resources Association* **34**, 73–89.

Deen, T. A., Arain, M. A., Champagne, O., Chow-Fraser, P., Nagabhatla, N. & Martin-Hill, D. 2021 Evaluation of observed and projected extreme climate trends for decision making in six nations of the Grand River, Canada. *Climate Services* **24** (2021), 100263.

Faramarzi, M., Abbaspour, K. C., Vaghefi, S. A., Farzaneh, M. R., Zehnder, A. J. B., Srinivasan, R. & Yang, H. 2013 Modeling impacts of climate change on freshwater availability in Africa. *Journal of Hydrology* **480**, 85–101.

Gassman, P. W., Reyes, M. R., Green, C. H. & Arnold, J. G. 2007 The soil and water assessment tool: historical development, applications, and future research directions. *Transactions of the ASABE* **50**, 1211–1250.

Ghimire, U., Srinivasan, G. & Agarwal, A. 2019 Assessment of rainfall bias correction techniques for improved hydrological simulation. *International Journal of Climatology* **39**, 2386–2399.

Giorgetta, M. A., Jungclaus, J., Reick, C. H., Legutke, S., Bader, J., Böttinger, M., Brovkin, V., Crueger, T., Esch, M., Fieg, K., Glushak, K., Gayler, V., Haak, H., Hollweg, H.-D., Ilyina, T., Kinne, S., Kornblueh, L., Matei, D., Mauritsen, T., Mikolajewicz, U., Mueller, W., Notz, D., Pithan, F., Raddatz, T., Rast, S., Redler, R., Roeckner, E., Schmidt, H., Schnur, R., Segschneider, J., Six, K. D., Stockhause, M., Timmreck, C., Wegner, J., Widmann, H., Wieners, K.-H., Claussen, M., Marotzke, J. & Stevens, B. 2013 Climate and carbon cycle changes from 1850 to 2100 in MPI-ESM simulations for the Coupled Model Intercomparison Project phase 5. *Journal of Advances in Modeling Earth Systems* **5**, 572–597.

Gosling, S. N., Taylor, R. G., Arnell, N. W. & Todd, M. C. 2011 A comparative analysis of projected impacts of climate change on river runoff from global and catchment-scale hydrological models. *Hydrology & Earth System Sciences* **15**, 279–294.

Gudmundsson, L., Bremnes, J. B., Haugen, J. E. & Engen-Skaugen, T. 2012 Technical note: downscaling RCM precipitation to the station scale using statistical transformations – a comparison of methods. *Hydrology & Earth System Sciences* **16**, 3383–3390.

Hargreaves, G. L., Hargreaves, G. H. & Riley, J. P. 1985 Agricultural benefits for Senegal River Basin. *Journal of Irrigation and Drainage Engineering* **111**, 113–124.

Hoekstra, A. Y., Chapagain, A. K., Aldaya, M. M. & Mekonnen, M. M. 2012 *The Water Footprint Assessment Manual: Setting the Global Standard*. Eartscan Publishers, Washington, DC, USA.

Hoffman, N. 2007 Canada's growing population and its environmental influence, 1956 to 2006. *EnviroStats* **1** (1), 8–15.

Kaur, B., Shrestha, N. K., Daggupati, P., Rudra, R. P., Goel, P. K., Shukla, R. & Allataifeh, N. 2019 Water security assessment of the grand river watershed in Southwestern Ontario, Canada. *Sustainability* **11**, 1883.

Kummu, M., Ward, P. J., de Moel, H. & Varis, O. 2010 Is physical water scarcity a new phenomenon? global assessment of water shortage over the last two millennia. *Environmental Research Letters* **5**, 034006.

Li, Z., Huang, G., Wang, X., Han, J. & Fan, Y. 2016 Impacts of future climate change on river discharge based on hydrological inference: a case study of the Grand River Watershed in Ontario, Canada. *Science of the Total Environment* **548–549**, 198–210.

Maurer, E. P. & Hidalgo, H. G. 2007 Utility of daily vs. monthly large-scale climate data: an intercomparison of two statistical downscaling methods. *Hydrology & Earth System Sciences Discussions* **4**, 3413–3440.

Maurer, E. P., Hidalgo, H. G., Das, T., Dettinger, M. D. & Cayan, D. R. 2010 The utility of daily large-scale climate data in the assessment of climate change impacts on daily streamflow in California. *Hydrology & Earth System Sciences* **14**, 1125–1138.

Miro, M. E., Groves, D. G., Catt, D., Miller, B. & Social, R. 2018 *Estimating Future Water Demand for San Bernardino Valley Municipal Water District*. RAND Corporation, Santa Monica, CA, USA. Available from: https:///www.rand.org/pubs/working_papers/WR1288.html.

Murdock, T., Cannon, A. & Sobie, S. 2013 *Statistical Downscaling of Future Climate Projections, Report KM170-12-1236, Pacific Climate Impacts Consortium, University of Victoria*. British Columbia, Canada. Prepared for Environment Canada.

Nielsen, K. 2022 Grand River Conservation Authority warns water levels are low despite recent rainfall. Global News, September 14, 2022. Available from: https://globalnews.ca/news/9129300/grand-river-conservation-authority-warns-water-levels-are-low-despite-recent-rainfall/.

Nimmo, J. R., 2009 Vadose water. In: *Encyclopedia of Inland Waters*, Vol. 1 (Likens, G. E., ed.). Elsevier, Oxford, UK, pp. 766–777.

Ohlsson, L. & Turton, A. R. 1999 *The Turning of A Screw: Social Resource Scarcity as A Bottle-Neck in Adaptation to Water Scarcity*. Occasional Paper Series, School of Oriental and African Studies Water Study Group, University of London, London, UK.

Parry, M., Canziani, O., Palutikof, J., van der Linden, P. & Hanson, C. 2007 *Climate Change 2007: Impacts, Adaptation and Vulnerability*. Report, Contribution of Working Group II to the Fourth Assessment Report of the Intergovernmental Panel on Climate Change (IPCC), Cambridge, UK.

Pastor, A., Ludwig, F., Biemans, H., Hoff, H. & Kabat, P. 2014 Accounting for environmental flow requirements in global water assessments. *Hydrology & Earth System Sciences* **18**, 5041–5059.

Riahi, K., Van Vuuren, D. P., Kriegler, E., Edmonds, J., O'neill, B. C., Fujimori, S., Bauer, N., Calvin, K., Dellink, R. & Fricko, O. 2017 The shared socioeconomic pathways and their energy, land use, and greenhouse gas emissions implications: an overview. *Global Environmental Change* **42**, 153–168.

Rodrigues, D. B., Gupta, H. V. & Mendiondo, E. M. 2014 A blue/green water-based accounting framework for assessment of water security. *Water Resources Research* **50**, 7187–7205.

Samir, K. C. & Lutz, W. 2017 The human core of the shared socioeconomic pathways: population scenarios by age, sex and level of education for all countries to 2100. *Global Environmental Change* **42**, 181–192.

Sanderson, M. 1993 Climate change and water in the great lakes basin. *Canadian Water Resources Journal/Revue Canadienne des Ressources Hydriques* **18**, 417–424.

Schewe, J., Heinke, J., Gerten, D., Haddeland, I., Arnell, N. W., Clark, D. B., Dankers, R., Eisner, S., Fekete, B. M. & Colón-González, F. J. 2014 Multimodel assessment of water scarcity under climate change. *Proceedings of the National Academy of Sciences* **111**, 3245–3250.

Schuol, J., Abbaspour, K. C., Srinivasan, R. & Yang, H. 2008 Estimation of freshwater availability in the West African sub-continent using the SWAT hydrologic model. *Journal of Hydrology* **352**, 30–49.

Shifflett, S. 2014 *Grand River Watershed Water Management Plan: Climate Change Scenario Modeling, Report*.Grand River Conservation Authority (GRCA), Ontario, Canada.

Shrestha, N. K. & Wang, J. 2018a Current and future hot-spots and hot-moments of nitrous oxide emission in a cold climate river basin. *Environmental Pollution* **239**, 648–660.

Shrestha, N. K. & Wang, J. 2018b Predicting sediment yield and transport dynamics of a cold climate region watershed in changing climate. *Science of the Total Environment* **625**, 1030–1045.

Shrestha, N. K., Du, X. & Wang, J. 2017 Assessing climate change impacts on fresh water resources of the Athabasca River Basin, Canada. *Science of the Total Environment* **601–602**, 425–440.

Statistically Downscaled Climate Scenarios (PCIC) 2014 University of Victoria. Available from: https://www.pacificclimate.org/data/statistically-downscaled-climate-scenarios

Taylor, K. E., Stouffer, R. J. & Meehl, G. A. 2012 An overview of CMIP5 and the experiment design. *Bulletin of the American Meteorological Society* **93**, 485–498.

Veettil, A. V. & Mishra, A. K. 2016 Water security assessment using blue and green water footprint concepts. *Journal of Hydrology* **542**, 589–602.

Veettil, A. V. & Mishra, A. K. 2018 Potential influence of climate and anthropogenic variables on water security using blue and green water scarcity, falkenmark index, and freshwater provision indicator. *Journal of Environmental Management* **228**, 346–362.

Voldoire, A., Sanchez-Gomez, E., y Mélia, D. S., Decharme, B., Cassou, C., Sénési, S., Valcke, S., Beau, I., Alias, A. & Chevallier, M. 2013 The CNRM-CM5. 1 global climate model: description and basic evaluation. *Climate Dynamics* **40**, 2091–2121.

Volodin, E. M., Dianskii, N. A. & Gusev, A. V. 2010 Simulating present-day climate with the INMCM4. 0 coupled model of the atmospheric and oceanic general circulations. *Izvestiya, Atmospheric and Oceanic Physics* **46**, 414–431.

Vörösmarty, C. J., Green, P., Salisbury, J. & Lammers, R. B. 2000 Global water resources: vulnerability from climate change and population growth. *Science* **289**, 284–288.

Wallace, J. S. 2000 Increasing agricultural water use efficiency to meet future food production. *Agriculture, Ecosystems & Environment* **82**, 105–119.

Wong, A. 2011 *Water Use Inventory Report for the Grand River Watershed, Report*.Grand River Conservation Authority, Cambridge, Ontario, Canada.

Zhang, B., Shrestha, N., Daggupati, P., Rudra, R., Shukla, R., Kaur, B. & Hou, J. 2018 Quantifying the impacts of climate change on streamflow dynamics of two major rivers of the Northern Lake Erie Basin in Canada. *Sustainability* **10** (8), 2897.

First received 26 September 2022; accepted in revised form 9 March 2023. Available online 22 March 2023